


# Effect of piston geometry on combustion characteristics of CI engine used Sal seed oil

International J of Engine Research  
2023, Vol. 24(7) 3157–3169  
© IMechE 2022  
Article reuse guidelines:  
sagepub.com/journals-permissions  
DOI: 10.1177/14680874221143405  
journals.sagepub.com/home/jer  


Ilker Temizer<sup>1</sup>  and Omer Cihan<sup>2</sup> 

## Abstract

The effect of piston bowl geometry on reducing soot emissions, improving combustion, and in-cylinder flow movements in a direct injection diesel engine was investigated. Standard combustion chamber (SCC) and newly modified combustion chamber (MCC) geometries were compared at the same compression ratio (17.5:1). Experimental analysis of diesel engines is expensive and time consuming, and therefore the Computational Fluid Dynamics program was used to analyze the combustion, flow and emission process. AVL Fire ESE Diesel software was used in the numerical study. The numerical work was compared with the experimental results, and it was validated. In addition, 10% biodiesel mixture (10% Sal seed oil methyl ester + 90% diesel fuel) and diesel fuel were used in the analysis. These fuels and two different bowl geometries were investigated at 2000 rpm and full load conditions. Thus, the effect of the used biodiesel fuel and the developed bowl geometry were investigated. Sal seed oil methyl ester was used as biodiesel fuel. The results show that higher turbulence velocity distribution, better mixture fraction values and lower soot formation distribution are obtained by directing the MCC type fuel according to SCC type. When the pressure, temperature and heat release in the combustion chamber are examined, the highest values were obtained with B10 blended fuel used at the SCC type combustion chamber. The maximum heat release rates are 8.72, 9.38, 8.21, and 9.30 J/° for SCCD100, SCCB10, MCCD100 and MCCB10 fuels, respectively.

## Keywords

Biodiesel, Sal seed oil methyl ester, piston bowl geometry, combustion, soot, diesel engine

Date received: 8 September 2022; accepted: 17 November 2022

## Introduction

In the world, oil prices are increasing and fossil fuel reserves are rapidly being depleted. In global marketplace is predicted that diesel fuel, which is among fossil fuels, will be partially replaced by biodiesel fuel. The used biodiesel fuel is suitable for the constructive of the engine and at the same time it is aimed to improve the exhaust emissions.<sup>1–5</sup> Today, many studies are on the engine characteristics of biodiesel fuels. In the studies conducted is evaluated that biodiesel fuel will be a good alternative fuel type to diesel fuel due to its direct use without structural changes in the engine and especially its environmental effects.<sup>6</sup> These studies based on short-term studies show that biodiesel fuel will be promising in future.<sup>7–13</sup>

Many studies are in the literature examining the effects of biodiesel fuels on combustion, performance and emissions in engine. Karami et al. was made that numerical analysis of combustion characteristics of a diesel engine fueled with diesel-tomato seed oil

biodiesel blends. The numerical study was done using AVL FIRE software. This study conducted with B0 (neat diesel), B5 (5% biodiesel + 95% diesel), B10 and B20 at different engine loads and speeds. As a result, the maximum temperature in-cylinder occurred at 15° ATDC. Also, the smallest and largest ignition delay was determined for B20 at about 8–9 °CA and for B10 at about 13 °CA, the highest heat release rate released at 1400 rpm at 20.5 °CA, and the highest and lowest of in-cylinder pressure were obtained at about 69 MPa in 2000 rpm and at about 65 MPa in 1600 rpm

<sup>1</sup>Department of Automotive Engineering, Sivas Cumhuriyet University, Sivas, Turkey

<sup>2</sup>Department of Mechanical Engineering, Hakkari University, Hakkari, Turkey

## Corresponding author:

Omer Cihan, Department of Mechanical Engineering, Hakkari University, Zeynel Bey Campus, Hakkari 30000, Turkey.  
Email: omercihan@hakkari.edu.tr

respectively.<sup>14</sup> In other study, 100% diesel and B10 (90% diesel 10% triacetin) fuels in the AVL Fire ESED program were tested by operating a diesel engine at different loads and 1500 rpm. This study was examined pre and post-injection-rate shapes on the combustion process. Thanks to the used biodiesel fuel, NO<sub>x</sub> emission has been reduced as it reduces the temperatures in the combustion chamber. As a result, NO<sub>x</sub>-soot trade-off was concluded to be considerably affected by the injection-rate shape in combustion process.<sup>15</sup> Asadi et al. tested a diesel engine by using the ESE Diesel part of the AVL Fire program. The engine was operated at 10% and 20% biofuel mixing ratios, 20% and 30% pilot injection, and two different injection times. Rapeseed-based biodiesel was used as biodiesel fuel. Looking at the results, ethanol combustion results in lower chamber temperature and subsequently lower NO<sub>x</sub> emissions than biodiesel combustion.<sup>16</sup> Hassan et al. analyzed that the effects on engine performance and emissions in a diesel engine fueled with biodiesel produced from Australian Beauty Leaf Tree. Biodiesel fuel was occurred at rates of 5% and 10%. Test engine was operated at different engine speeds and full throttle. As a result, B10 fuel according to diesel fuel was been seen to slightly improve engine performance while slightly reducing emissions.<sup>17</sup> In another study, 5%, 10%, and 20% tomato seed oil were added to diesel fuel. Test engine was operated at 0%, 25%, 50%, 75%, and 100% of full load of the engine and engine speeds from 1200 to 2400 rpm at increments of 200 rpm. As the biodiesel ratio and engine speed increased, a reduction in specific fuel consumption and torque, high NO<sub>x</sub> emission and lower CO, CO<sub>2</sub> and soot emissions were achieved. Also, the best results in performance and emissions were obtained at 10% fuel mixture ratio.<sup>18</sup> Aksoy et al. investigated the effect of different proportions of neutralized waste cooking oil biodiesel mixture on combustion, performance and emissions in a single-cylinder and direct injection diesel engine at different loads. The mixing ratio of biodiesel fuel was 30%. As a result of, biodiesel fuel compared to neat diesel fuel, the in-cylinder pressure and heat release rates were increased because of better oxidation reactions, and it obtained with higher indicated mean effective pressure.<sup>19</sup> Salehian and Shirneshan performed to analyze the NO<sub>x</sub> conversion efficiency on a single-cylinder engine by using AVL FIRE software. In this study used E20B50D30 (20% ethanol, 50% biodiesel, 30% diesel) D100, E10D90, E20D80, B25D75, and B50D50 fuel blends. The engine operated at engine speeds of 1800, 2150, and 2500 rpm under full load. As a result, lower NO<sub>x</sub> emissions were achieved in all fuel blends and 2500 rpm engine speed.<sup>20</sup> Farajollahi and Firuzi reported that AVL Fire software used for improving the fuel spray characteristics and diesel engine performance. Microscopic and macroscopic diesel and the biodiesel fuel spray characteristics investigated in this study. Research showed that the biodiesel spray was bigger cone angle and smaller penetration length.<sup>21</sup>

Lešnik et al. focused on simulating the fuel-spray development during different stages of the injection process by using the AVL FIRE 3D CFD program. Used biodiesel was produced from rapeseed oil at Biogoriva, Race, Slovenia that conformed to European standard EN 14214 and test engine operated at full load and different engine speeds. As a result, the spray penetration depth in the chamber was increased due to the properties of biodiesel such as higher density, sound velocity, spray pressure and bulk modulus.<sup>22</sup> In another study; using different mixing ratios of diesel, biodiesel or diesel and biodiesel, a direct injection single-cylinder diesel engine was numerically evaluated in the AVL Fire program. Diesel, B10 (10% rapeseed oil + 90% diesel), B20, and B50 fuels used. It had been determined that the temperature and pressure values in the combustion chamber decrease as the biodiesel ratio increases.<sup>23</sup> Ni et al. worked that characteristics of spray, combustion, and soot emissions of the diesel engine fueled with biodiesel-diesel blends and diesel were numerically modeled by using AVL-FIRE software. B10, B20, B50 and diesel fuels were used in test engine. Consequently, as the percentage of biodiesel fuel in the blend increased, the ignition timing advances, which helps to reduce soot formation. Also, the equivalence ratio of biodiesel fuels was lower than diesel fuel except at the end of injection. This state caused tendency of soot.<sup>24</sup> Some work has been done on the production of Sal (*Shorea robusta*) seed oil as biodiesel fuel. *Shorea robusta* is known as the Sal tree. It is an 18–30 m high deciduous plant belonging to the Dipterocarpaceae family.<sup>25,26</sup> Sal tree is located in the forests of South and Southeast Asia, covering approximately 14 million hectares of India, Bangladesh and Nepal.<sup>27</sup> Sal seeds were available at low cost. Sal seed could be produced as biodiesel and used in engine. Higher cetane ratio, oxidation stability and calorific value of Sal seed biodiesel had a curative effect on engine performance. In addition, the heating value of Sal seed and oil was 17.99 and 41.61 MJ/kg, respectively.<sup>28</sup> On the other hand, cold weather pours point and lowers cold filter plugging point (CFPP) values are a disadvantage for this biodiesel fuel.<sup>29,30</sup> Vedaraman et al. worked on biodiesel produced from Sal oil into Sal oil methyl ester (SOME) and its performance in direct injection diesel engine. SOME fuel compared to diesel, CO, HC, and NO<sub>x</sub> exhaust emission values were reduced by 25%, 45%, and 12% respectively. In addition, there was no significant change in thermal efficiency.<sup>30</sup> Pali and Kumar investigated the effect of Sal methyl ester (SME) and its mixture with diesel fuel in different proportions on performance, and combustion characteristics in a four-stroke and single-cylinder diesel engine. SME10, SME20, SME30, SME40, and D100 fuels had been tested. The highest cumulative heat release rate was achieved with SME10 fuel. The total combustion duration was calculated in the range of 0.05–0.95. As the rate of SME increases in diesel, the combustion occurs earlier in the first stage and the ignition delay

was shortened. Also, the engine was operated more smoothly.<sup>31</sup> Pali and Kumar focused on compared Sal Methyl Ester and Kusum Methyl Ester biodiesel fuels with each other. A single-cylinder, four-stroke, and water-cooled diesel engine was operated at 1500 rpm and injection pressures in the range of 200–205 bars. Sal methyl ester showed higher performance than kusum methyl ester.<sup>32</sup>

Another way to improve combustion and performance in the engine is through the combustion chamber geometry. In a study, lateral swirl combustion system was designed and traditional  $\omega$  type combustion system was developed. An interaction mechanism was established between the lateral swirl combustion chamber and the spray jet. The study, which was examined experimentally and numerically, consequently reduced fuel consumption and soot emission depending on the injection angle with this combustion chamber geometry. Thermal efficiency and combustion performance were increased with this combustion chamber geometry.<sup>33</sup> Sener et al. examined the performance, emission values and combustion characteristics of the piston by examining five different bowl shapes of the piston with the CFD program. Piston bowl geometry has a great impact on heat release, in-cylinder temperature and pressure, and emissions. DE and DF bowl designs showed better combustion characteristics and lower emission values than other designs.<sup>34</sup> The combustion law that provides optimum combustion for the 3LD510 direct injection diesel engine was issued and the MR-1 combustion chamber piston was designed. With the piston design, an increase of 9.6% in power, an 8.7% reduction in specific fuel consumption and a 30% reduction in soot emission were detected.<sup>35</sup> Approximately the same power was achieved with this engine at lower in-cylinder pressure. As the pressure decreases, the strain is less, NOx emissions was decreased due to in-cylinder temperature decreased.<sup>36</sup> The MR combustion mechanism, realized in a double turbulent vortex combustion environment, combines the advantages of both Diesel and Otto cycles in a single structure.<sup>37,38</sup> Ganji et al. modeled hemispherical combustion chamber (HCC), shallow depth combustion chamber (SCC) and Toroidal combustion chamber (TCC) geometries in compression ratio of 17.5 using Converge simulation. A better air-fuel mixture and homogeneous mixture was provided with TCC geometry. The most suitable combustion chamber geometry was determined for 1.26 mm piston bowl depth.<sup>39</sup> In another similar study, three different piston bowl geometries (Toroidal Re-entrant Combustion Chamber (TRCC), TCC and HCC) and four different spray angles (150°, 155°, 160° and 165°) were used. It was emphasized that mixture formation, fuel consumption and soot emissions became better with TRCC type geometry and 160° spray angle.<sup>40</sup> Li et al. evaluated that LSCS (Lateral Swirl Combustion Systems) and DSCS

(Double Swirl Combustion Systems) were analyzed using the AVL Fire program. Fuel consumption and soot emissions were reduced with LSCS geometry.<sup>41</sup> Wei et al. proposed a new swirl formation to improve spray dispersion, improve mix quality, and increase air-flow movement in the combustion chamber. In the modeling with AVL Fire, better engine performance was obtained with the new combustion chamber geometry, where NOx and soot emissions at the rate of 0.8 swirl.<sup>42</sup>

There are many studies on the use of biodiesel fuel at different rates and the effect of different combustion chamber geometries in diesel engines. Diesel blended fuels which containing biodiesel at certain proportions are used in engines without the need for any modification.<sup>43</sup> These blends show characteristic combustion characteristics similar to petroleum diesel. Increasing of biodiesel ratio in the mixture could cause significant power and performance losses and negative effects on engine lubricating oil.<sup>9,17,44–49</sup> Therefore, it is very important use of blends containing biodiesel at certain proportions in terms of engines.

In this study, direct injection, air-cooled and single-cylinder diesel engine was numerically investigated using AVL Fire. Diesel fuel was used in the engine and 10% Sal seed oil methyl ester was added to the diesel fuel. The aim of the study was to investigate the effects of Sal seed oil biodiesel on the standard combustion chamber (SCC) and a new modified combustion chamber (MCC) geometries. In numerical study, it was investigated what effect it provide in the engine by making detailed combustion analysis and in-cylinder flow motion. All features of the engine were kept constant except for the piston in order to fully understand the effect of combustion chamber geometry and biodiesel fuel on the engine parameters.

## Material and methods

### Experimental study

In this study, engine performance characteristics and in-cylinder pressure/crank angle data of ANTOR 3 LD 510 diesel engine were determined. Schematic representation of the experimental setup is given in Figure 1. The engine was operated at 2000 rpm and full load, where the maximum torque was obtained. In the experimental results, the combustion analysis of the engine was carried out using the Febris combustion analysis program. Febris combustion analysis program recorded in-cylinder pressures and indicator diagram for at least 350 cycles for each test point. The cycle closest to the mean was selected by taking the average of these cycles. Cylinder pressure was measured using Oprant optical pressure sensor, and crank angle was measured using KUBLER encoder. Engine technical specifications are given in Table 1.

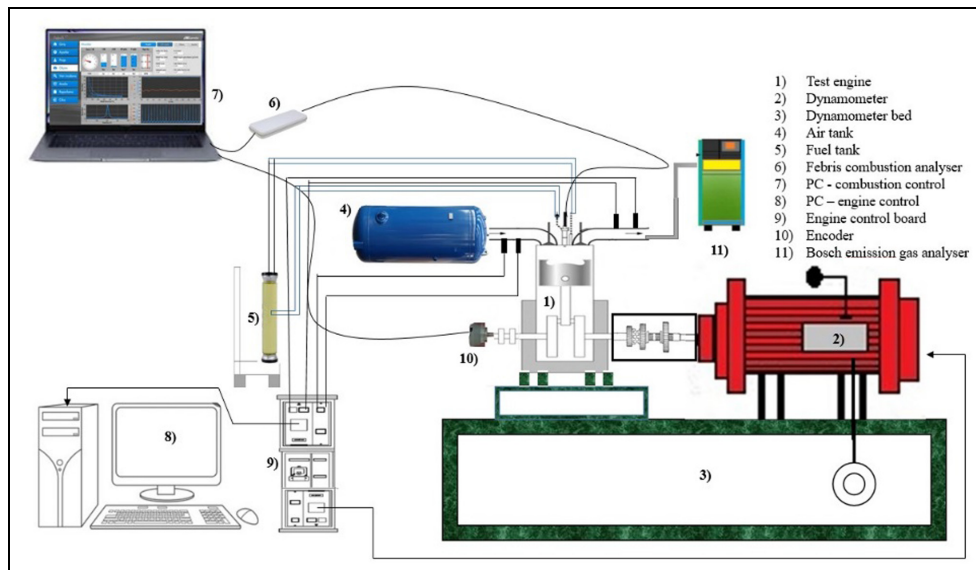


Figure 1. Schematic representation of the test setup.

Table 1. Engine technical specifications.

Engine type	ANTOR 3LD510 diesel engine, Single-cylinder, 4 stroke, direct injection
Type of cooling	Air-cooled
Bore × Stroke	85 × 90 (mm × mm)
Cylinder volume	510 cm <sup>3</sup>
Compression ratio	17.5
Crank radius	42 mm
Maximum power	6.6@3000 (kW)
Maximum torque	32.8@2000 (Nm)
Number of injection nozzle	4
Injection spray angle	126°

### Numerical Study

In this study, a numerical study was performed in the AVL Fire ESE Diesel section using the properties of a real diesel engine. The optimum value among 50,000, 100,000, and 120,000 cells was obtained in 100,000

mesh number. In Figure 2, similar results were obtained between numerical analysis results obtained from numerical modeling and experimental results. When verifying the combustion characteristics with experimental results, in-cylinder pressure and heat release rate are usually compared. There are many studies in the literature on this subject.<sup>14,50–52</sup> The type of combustion chamber used in the comparison is SCC (Figure 2). In Figure 3, close to results were obtained between numerical analysis and experimental results. These results also show the results obtained in real engine modeling. Simulation models and initial boundary conditions are given in Table 2. Properties and equations of these models are preferred and accepted in many numerical studies.<sup>44,53,54</sup> Seed oil methyl ester was chosen as the biodiesel fuel. The chemical content of this fuel was defined in AVL FIRE and mixed with 10% of diesel fuel as volume. This ratio has been chosen as it is accepted in the literature and is an optimum ratio in terms of engine performance and emissions. The fatty acid composition and physicochemical properties of Sal

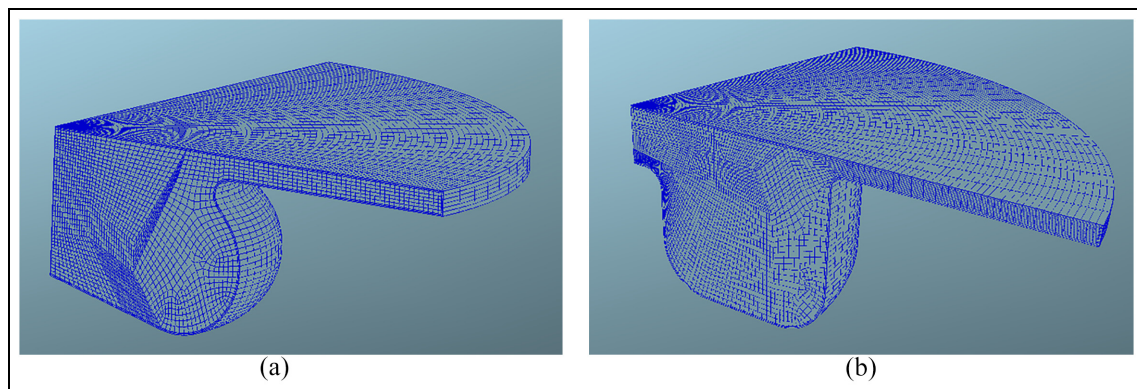
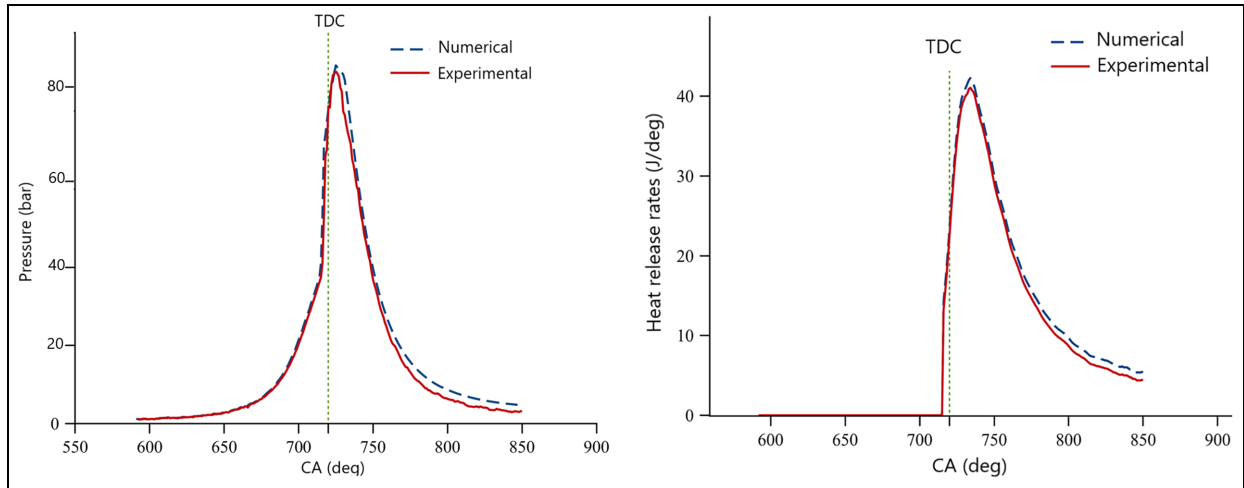


Figure 2. Computational grid of (a) MCC and (b) SCC piston bowl geometry at TDC.



**Figure 3.** The pressure/crank angle and heat release rate/crank angle changes in D100 fueled operation, experimentally and numerically.

**Table 2.** Modeling used in numerical analysis and initial boundary conditions.

Combustion model	ECFM-3Z
Breakup model	Wave
Turbulence model	K-zeta-f model
Wall interaction model	Walljet1
Evaporation model	Multi component
Soot emission model	Kinetic model
Injection Timing (start and stop)	705° and 729° (CA)
Injection rate (mass)	5.11e-6 kg
Engine speed	2000 rpm
Air inlet temperature	293.15 (K)
Air inlet pressure	1 (bar)
Fuel injection temperature	330.15 (K)

seed oil methyl ester<sup>55</sup> were described to AVL Fire software. The calculations were carried out at approximately 100,000 finite volume elements for both combustion chambers (Figure 2).

The ECFM-3Z model solves transport equations to determine the average amounts of chemical products (O<sub>2</sub>, N<sub>2</sub>, CO<sub>2</sub>, CO, H<sub>2</sub>, H<sub>2</sub>O, O, H, N, OH, and NO) formed at the end of combustion. Average amounts are calculated for each cell separately. In the calculation of these amounts, both burned gases and unburned fuel and air mixtures are included,

$$\frac{\partial \rho y_x}{\partial t} + \frac{\partial \rho u y_x}{\partial x_i} - \frac{\partial}{\partial x_i} \left( \left( \frac{\mu}{s_c} + \frac{\mu_t}{s_t} \right) \frac{\partial y_x}{\partial x_i} \right) = \omega_x$$

Here,  $\omega_x$  represents the source term for combustion, and  $y_x$  represents the mass ratios for the species.

It should be noted that this model also includes the pollutant emissions model.

Turbulent viscosity;

$$v_t = C_\mu \xi k T$$

Turbulent kinetic energy;

$$\frac{\partial k}{\partial t} + U_j \frac{\partial k}{\partial x_j} = P_k - \varepsilon + \frac{\partial}{\partial x_j} \left[ \left( v + \frac{v_t}{\sigma_k} \right) \frac{\partial k}{\partial x_j} \right]$$

Turbulence kinetic energy dissipation rate;

$$\frac{\partial \varepsilon}{\partial t} U_j \frac{\partial \varepsilon}{\partial x_j} = \frac{C_\varepsilon 1 P_k - C_\varepsilon 2}{T} + \frac{\partial}{\partial x_j} \left[ \left( v + \frac{v_t}{\sigma_\varepsilon} \right) \frac{\partial \varepsilon}{\partial x_j} \right]$$

Velocity scale;

$$\frac{\partial \xi}{\partial t} U_j \frac{\partial \xi}{\partial x_j} = f - \frac{\xi}{k} P_k + \frac{\partial}{\partial x_j} \left[ \left( v + \frac{v_t}{\sigma_\xi} \right) \frac{\partial \xi}{\partial x_j} \right]$$

Elliptical relief factor;

$$L^2 \nabla^2 f - f = \frac{1}{T} \left( C_1 - 1 + C_2 \frac{P_k}{\varepsilon} \right) \left( \xi - \frac{2}{3} \right)$$

### Turbulent kinetic energy generation

$$P_k = \frac{\partial U_j}{-u_i u_j \partial z_i}$$

$$P_k = v_t S^2$$

Many parameters of turbulence formation are solved in detail with the k- $\xi$ -f module. The constants of the k- $\xi$ -f module are given below.<sup>56</sup>

$$C_\mu = 0.22, \sigma_k = 1, \sigma_\varepsilon = 1.3, \sigma_\xi = 1.2, C_\varepsilon = 1.2,$$

$$C_\varepsilon 1 = 1.4 \left( 1 + \frac{0.012}{\xi} \right), C_\varepsilon 2 = 1.9, C_1 = 1.4$$

$$C_2 = 0.65, C_T = 6, C_L = 0.36, C_\eta = 85$$

The liquid jet is described in two ways. The first of these is the primary break-up. In this mechanism, the number of droplets, size, propagation, and dispersion

of the liquid jet are studied. In the second mechanism, droplets in dispersed small groups are examined. Droplet size is very important for this dispersion and is a characteristic size. In fact, in both mechanisms, liquid propagation and droplet properties depend on the properties of the liquid itself and the properties of the surrounding gas. The second dispersion model examines the droplet aerodynamic properties depending on the change in Weber number ( $We$ ). There  $u$  is the velocity,  $d$  is the orifice diameter,  $\rho$  is the density of the liquid, and  $\sigma$  is the surface tension of the liquid.

$$We = u^2 \rho d / \sigma$$

## Results and discussion

The combustion characteristics of diesel engine used Sal seed oil methyl ester biodiesel was conducted and compared with diesel operation. In this study, the effect of different fuel mixture on MCC and SCC combustion chamber geometries was investigated. The full load operating condition was used to simulate the geometries at a constant engine speed of 2000 rpm.

### Combustion characteristics

In-cylinder pressure directly affects engine characteristics, and it is very important for analyzing combustion behavior. The change in the in-cylinder gas pressure concerning the crank angles for biodiesel fuel blend and two different chamber geometry was given in Figure 3. In both combustion chamber geometries, the biodiesel fuel obtained a higher in-cylinder pressure than the reference diesel fuel. Because of the low evaporation degrees of biodiesel fuels compared to diesel fuel, it becomes difficult for the fuel to ignite in the combustion chamber. Therefore, it was thought that it caused an increase in maximum pressures due to the prolongation of the ignition delay (ID) duration. In general, the high density of biodiesel fuel compared to diesel fuel means more fuel atomization into the combustion chamber per unit time. These high-density fuel particles accumulated during the ID especially increase the severity of uncontrolled combustion and may cause a maximum pressure increase. This situation was particularly evident after the top dead center (TDC). Here, another parameter to be compared is the shape of the combustion chamber. For both diesel and biodiesel fuels, lower maximum pressures were obtained in the MCC combustion chamber compared to the SCC combustion chamber (Figure 4). A slower burning period was the reason for obtaining lower in-cylinder pressure with the newly developed combustion chamber geometry. In addition, better plastering and earlier evaporation were achieved compared to SCC.<sup>51</sup> The MCC type compared to the SCC type, it had been observed in the combustion analysis that the mixture was more

homogeneous in the combustion chamber due to its special geometric bowl structure. For both types of fuels, thanks to the bowl geometry of the MCC combustion chamber, it was observed that it increased the contact of the fuel with the surface in areas close to the surfaces, facilitating evaporation, and thus contributes to the reduction of in-cylinder peak pressures. Another flow analysis that supported this result is the turbulence velocities of the air/fuel fluids in the combustion chamber. MCC compared to SCC type, mixing formation velocity increased thanks to its bowl structure. Diesel combustion temperature values were calculated from instantaneous in-cylinder pressure, cylinder volume and airflow rate. In-cylinder temperatures of biodiesel and diesel fuel at 2000 rpm engine speed were shown in Figure 4. The SCC bowl geometry achieved higher cylinder temperature than MCC type. On the other hand, the engine operating with biodiesel reached a higher in-cylinder temperature than reference diesel fuel (Figure 4). This situation can be explained by the presence of extra oxygen molecules in biodiesel fuel, which facilitates the complete combustion of the fuel. Similar behavior is reported by Dueso et al.<sup>57</sup> Moreover, physical properties such as high cetane number, viscosity, and density contributed to the development of the combustion process.

Looking at Figure 4 helps us to understand the amount of heat energy that can be converted to useful work during fuel combustion. The net heat release rate (NHRR) mainly depends on the injection timing and ignition delay duration. When the NHRR results were examined for both the biodiesel blended fuel and the engine with different combustion chamber geometries, it was seen that similar results were obtained with the start of combustion (at 705 °CA). This state was seen that the differences during the combustion after the ignition delay more specifically occur. This was a result of the combustion characteristic of the fuel. It may be due to the higher specific heat of the B10 fuel, which needs more heat energy to evaporate in the cylinder by absorbing the heat from the combustion chamber.<sup>58</sup>

Especially with the combustion phenomena that started around the 729 °CA where the spraying ended, it was observed that the NHRR values formed a curve parallel to the pressure values (Figure 4). Biodiesel fuel mix reached higher NHRR values than diesel fuel. A higher NHRR was obtained in SCC with 10% biodiesel fuel. This result can be said to be because biodiesel fuel is more difficult to mix and therefore needs more duration for mixing.<sup>59</sup>

Combustion parameters (pressure, temperature, instantaneous and cumulative heat release rates) were higher with biodiesel mixture. A lower evaporation degree with a biodiesel blend has better physical properties (high cetane number, viscosity, and density). Therefore, combustion can be improved by using this fuel mixture in low power diesel engines and heavy duty engines.



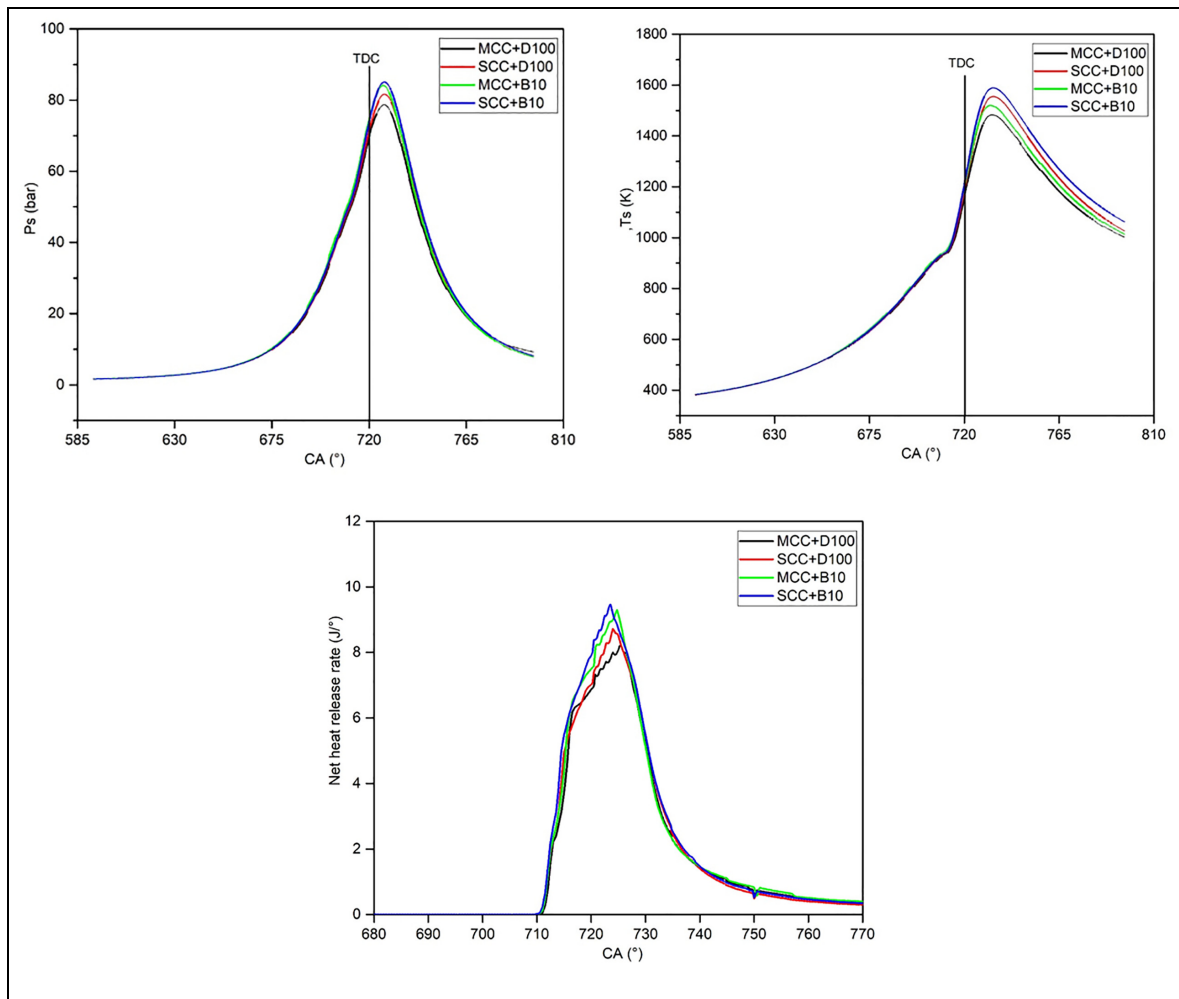


**Figure 4.** Variation of in-cylinder pressure, in-cylinder temperature and net heat release rate with crank angle in different combustion chamber geometries and fuel mixtures.

#### Variation of flow motion in different combustion chamber geometries and biodiesel fuel

The homogeneous distribution of the fuel-air mixture is very important for better combustion in diesel engines.<sup>60,61</sup> Another important parameter in the formation of air-fuel mixture is the turbulence velocity in the combustion chamber. Figures 5 and 6 shows turbulence velocity distributions of different combustion chamber geometries. It was seen that the MCC combustion chamber bowl structure increased the air/fuel mobility in the cylinder. This distribution was also reflected in the fuel/air mixture formation distributions. Especially when the piston was at the TDC, it was seen that both fuels had been plastered more on the wall in MCC type. This situation it's caused to evaporate more easily and form a better mixture air/fuel. Especially in the initial stages of fuel injection (for 710 °CA), it is seen that the fluid has a high turbulence speed compared to other crank angles, but with the mixture with air over time, the speed of the fuel particles decreases.<sup>51</sup> It was seen that this effect is distributed over a larger area with the advancement of the piston. Especially

when different combustion chambers were analyzed, it had been observed that the fluid hitting the cavity area in the MCC type combustion chamber had a higher turbulence velocity. As a result of the large area of turbulence, the laminar flame velocity also increased in this chamber geometry.<sup>62</sup> The turbulence velocities of the fluid and the mixing formations were parallel to each other. It was seen that its effect in the maximum area especially around 720 °CA and this value decreased in both combustion chambers as the volume increases.

Figures 7 and 8 shows the mixture fraction values for different crank angles. The MCC type compared to SCC type, there was a distinct difference in mixture formation especially at 729 °CA (the angle where the spraying ended) and afterward. It is very important to use fuels with high evaporation degree such as biodiesel fuel in different combustion chambers. The increase in the surface area of the fuel in contact with the wall, especially depending on the bowl geometry, significantly affected the formation of the mixture. This situation was more clear at 720 °CA and 730 °CA of the Figure 8. These results were thought to significantly

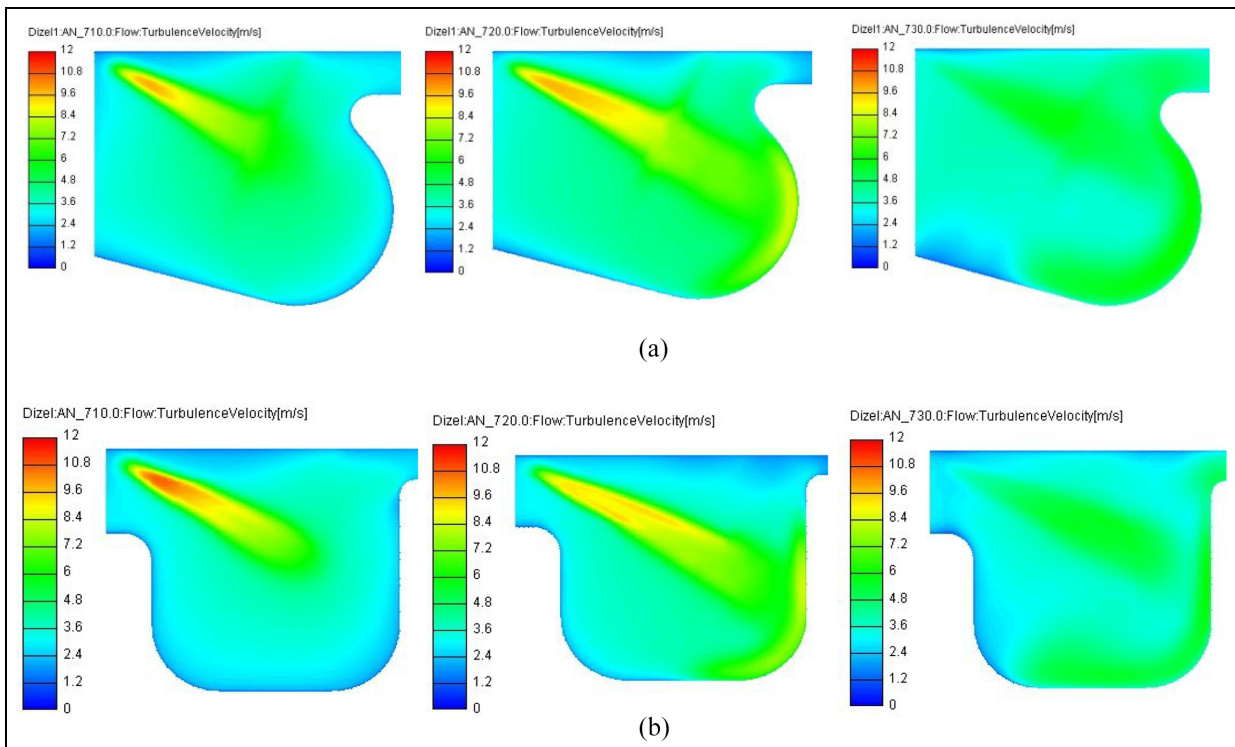


Figure 5. Flow turbulence velocity distribution of (a) MCC and (b) SCC chamber geometries for diesel fuel.

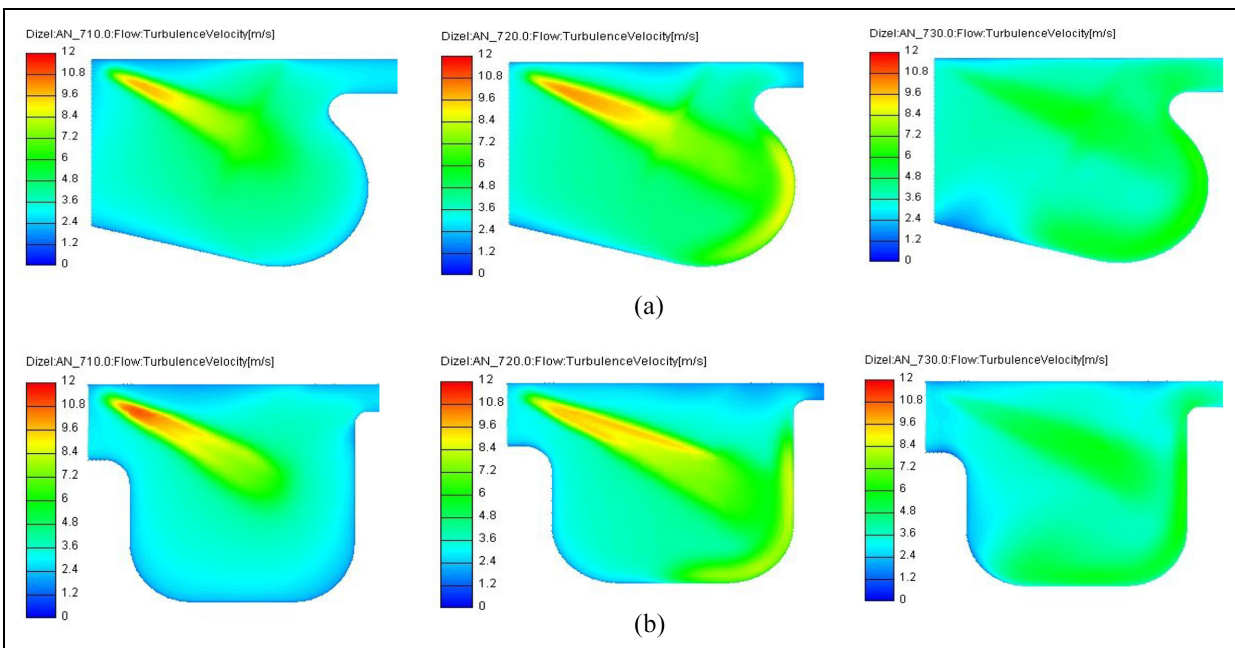


Figure 6. Flow turbulence velocity distribution of (a) MCC and (b) SCC chamber geometries for biodiesel fuel.

contribute to the use of alternative fuels in different combustion chambers.

In both combustion chamber models, it was seen that the mixture formation was concentrated in the bowl area where the fuel was sprayed and the geometry of this region was very important. Mixture formation is a factor that directly affects exhaust emissions as well as

engine performance values. Soot formation is a harmful emission type that occurs as a result of incomplete combustion of the hydrocarbon fuel component. C and H atoms are formed as a result of the decomposition of the sprayed fuel under the effect of the heat in the combustion chamber. Therefore, the formation of soot is actually a stage of combustion. Soot emission decreases



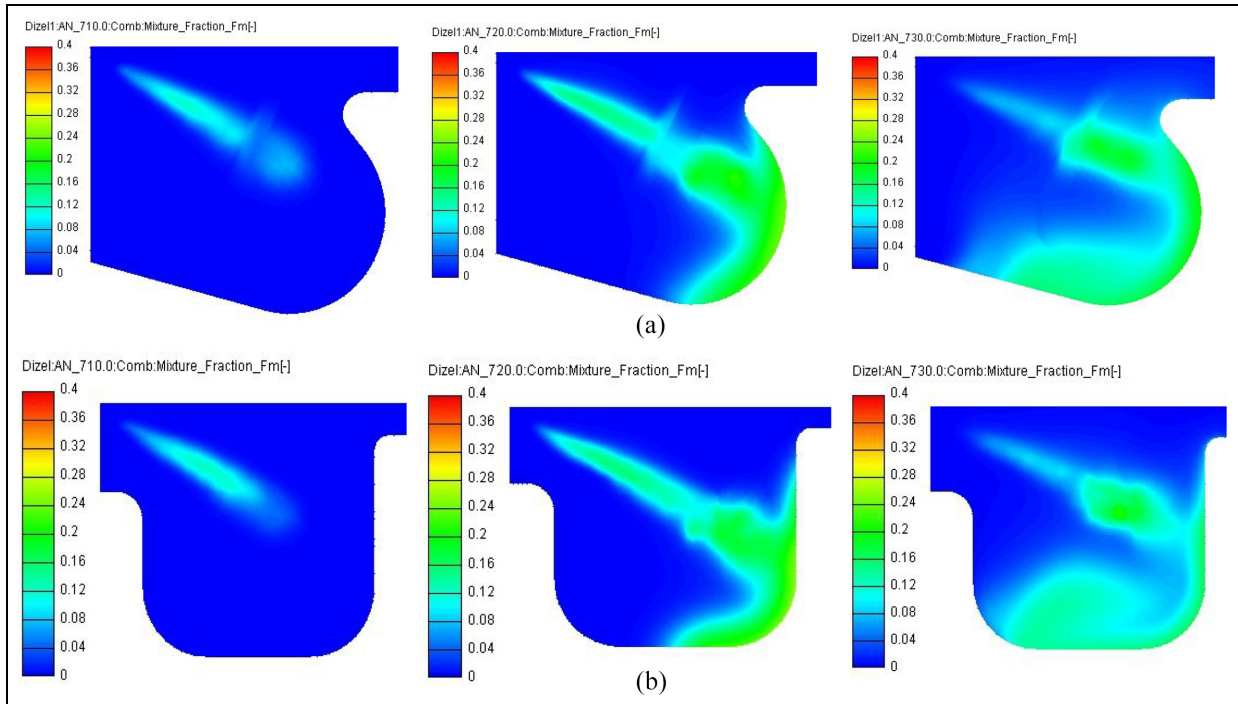


Figure 7. Mixture fraction values of MCC (a) and SCC (b) chamber geometries for diesel fuel.

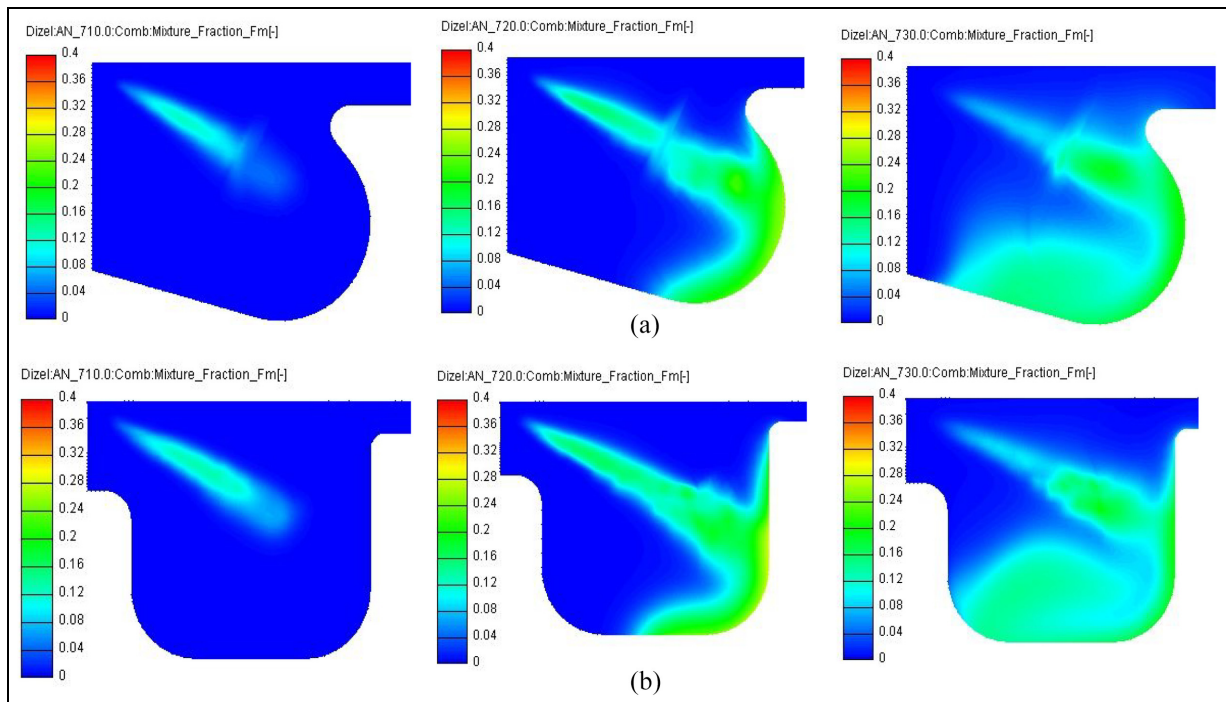


Figure 8. Mixture fraction values of MCC (a) and SCC (b) chamber geometries for biodiesel fuel.

as a result of the reaction of the decomposition C atoms with enough oxygen. When Figures 9 and 10 is examined, it is seen that soot formation is concentrated in the bowl area for both fuels. The presence of fuel in this area and soot emission in the heterogeneous mixture area was higher than in other areas. C atoms that do not react with sufficient temperature and oxygen at the end of the expansion stroke had been found to increase

soot emissions. The oxygen content of biodiesel fuel positively affects combustion. However, biodiesel fuel compared to diesel fuel, its high viscosity and C number caused an increase in soot emissions. Another parameter was the shape of the combustion chamber. The MCC type according to SCC type, it caused a reduction in soot emissions due to mixture formation and in-cylinder air mobility for both fuel types. Moreover, the

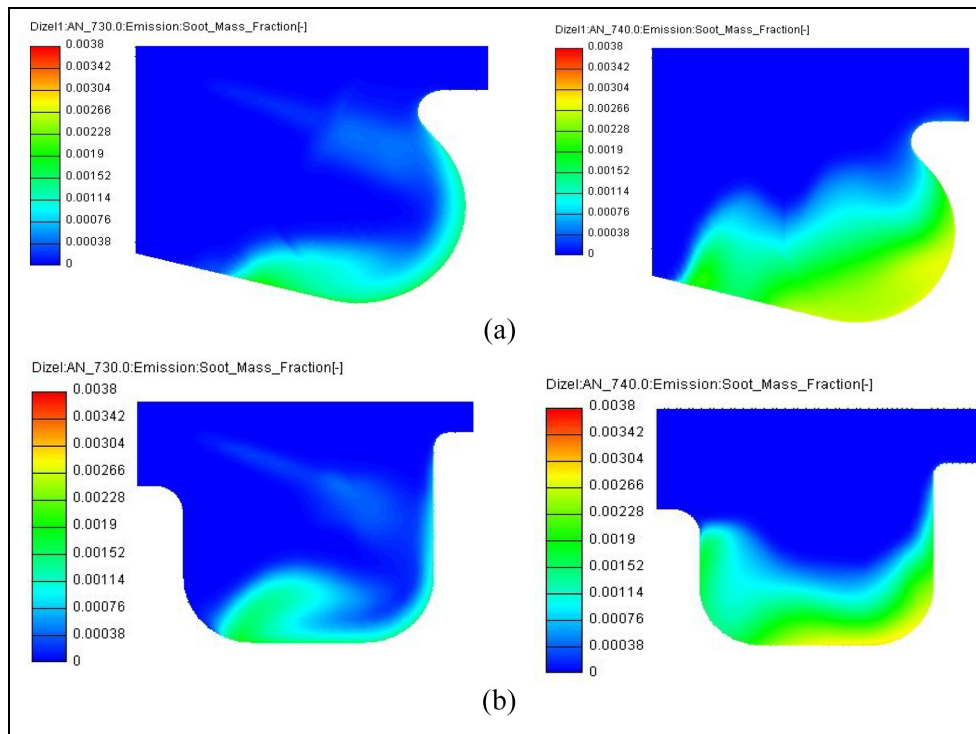


Figure 9. Soot formation distribution of MCC (a) and SCC (b) chamber geometries for diesel fuel.

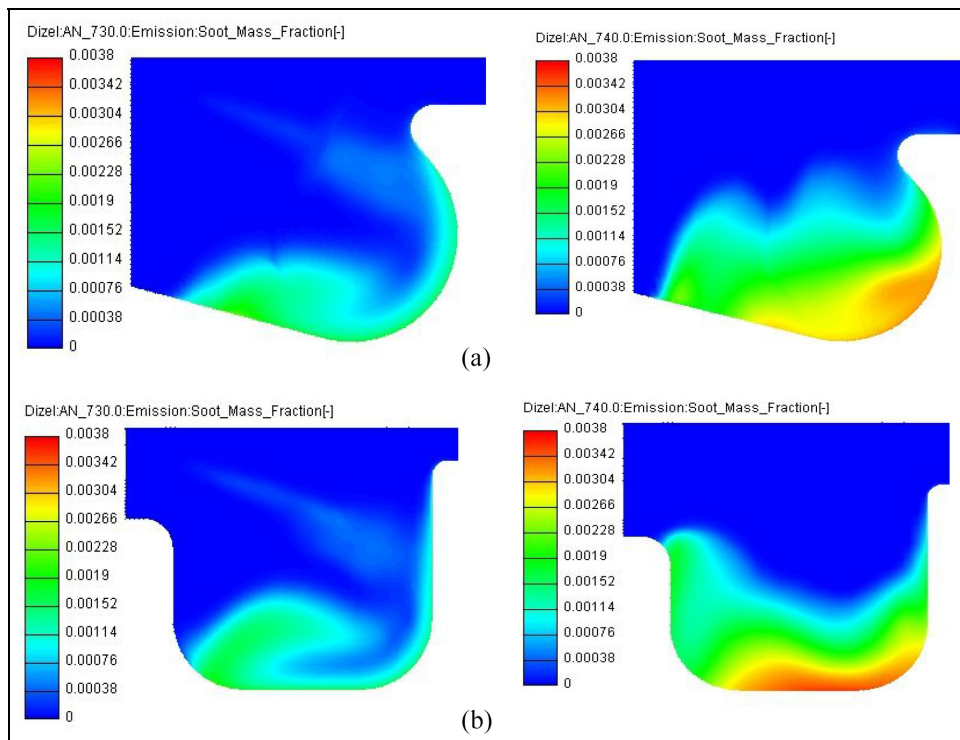


Figure 10. Soot formation distribution of: MCC (a) and SCC (b) chamber geometries for biodiesel fuel.

soot formation near the cylinder wall was reduced with guiding the air-fuel mixture motion toward the center of the cylinder.<sup>63</sup>

Biodiesel blend ratio is more suitable for complete combustion thanks to the high oxygen it contains.

Therefore, it can be said that CO<sub>2</sub> emissions decrease and reduce greenhouse gases. In addition, when this biodiesel blend is used with MCC geometry, C emissions have decreased, which can be said to reduce the formation of greenhouse gases.

## Conclusions

This study dealt with the simulation of the combustion characteristics of a DI diesel engine fueled with biodiesel produced from Sal seed oil methyl ester is investigated, and SCC and MCC combustion chamber geometries. Moreover, the effects of turbulence velocity distribution, mixture fraction and soot formation parameters were numerically investigated. The numerical results demonstrated that the maximum pressures increased as a result of the prolongation of the ID duration due to the high heat of evaporation of biodiesel fuel mixture compared to neat diesel. In-cylinder temperature and net heat release rate increased because of oxygen molecules in biodiesel fuel, and physical properties such as high cetane number, viscosity and density. In addition, the maximum heat release rates were 8.72, 9.38, 8.21, and 9.30 J/° for SCCD100, SCCB10, MCCD100 and MCCB10 fuels, respectively. On the other hand, the MCC combustion chamber slightly decrease maximum pressure and temperature was observed due to improvement of mixture formation near the wall. Maximum in-cylinder pressure values found 81.6, 85.07, 78.66, and 84.11 bar for SCCD100, SCCB10, MCCD100 and MCCB10 fuels, respectively. MCC geometry according to SCC was provided a more homogeneous mixture in terms of mixture fraction and turbulence velocity. Lower soot emissions were observed in the MCC geometry compared to the SCC.

## Acknowledgement

Part of this study was supported by the Scientific and Technological Research Council of Turkey (TUBITAK) within the scope of project 120M143


## Declaration of conflicting interests


The author(s) declared no potential conflicts of interest with respect to the research, authorship, and/or publication of this article.

## Funding

The author(s) received no financial support for the research, authorship, and/or publication of this article.

## ORCID iDs

Ilker Temizer  <https://orcid.org/0000-0003-1170-3898>

Omer Cihan  <https://orcid.org/0000-0001-8103-3063>

## References

- Acharya N, Nanda P, Panda S and Acharya S. Analysis of properties and estimation of optimum blending ratio of blended mahua biodiesel. *Eng Sci Technol Int J* 2017; 20: 511–517.
- Milano J, Ong HC, Masjuki HH, et al. Optimization of biodiesel production by microwave irradiation-assisted transesterification for waste cooking oil-Calophyllum inophyllum oil via response surface methodology. *Energy Convers Manag* 2018; 158: 400–415.
- Murillo S, Míguez JL, Porteiro J, Granada E and Morán JC. Performance and exhaust emissions in the use of biodiesel in onboard diesel engines. *Fuel* 2007; 86(12-13): 1765–1771.
- Hwang J, Qi D, Jung Y and Bae C. Effect of injection parameters on the combustion and emission characteristics in a common-rail direct injection diesel engine fueled with waste cooking oil biodiesel. *Renew Energy* 2014; 63: 9–17.
- Damanik N, Ong HC, Chong WT and Silitonga AS. Biodiesel production from *Calophyllum inophyllum*–palm mixed oil. *Energy Sources A Recovery Util Environ Eff* 2017; 39: 1283–1289.
- An H, Yang WM, Maghbouli A, et al. Numerical investigation on the combustion and emission characteristics of a hydrogen assisted biodiesel combustion in a diesel engine. *Fuel* 2014; 120: 186–194.
- Staat F and Gateau P. The effects of rapeseed oil methyl ester on diesel engine performance exhaust emissions and long-term behavior—a summary of three years of experimentation. *SAE paper 950053*, 1995, pp.1–9. DOI: 10.4271/950053
- Canakci M, Erdil A and Arcaklioğlu E. Performance and exhaust emissions of a biodiesel engine. *Appl Energy* 2006; 83(6): 594–605.
- Ganapathy T, Gakkhar RP and Murugesan K. Influence of injection timing on performance, combustion and emission characteristics of *Jatropha* biodiesel engine. *Appl Energy* 2011; 88: 4376–4386.
- Solaimuthu C, Ganesan V, Senthilkumar D and Ramasamy KK. Emission reductions studies of a biodiesel engine using EGR and SCR for agriculture operations in developing countries. *Appl Energy* 2015; 138: 91–98.
- Wong KI, Wong PK, Cheung CS and Vong CM. Modeling and optimization of biodiesel engine performance using advanced machine learning methods. *Energy* 2013; 55: 519–528.
- Ghobadian B, Rahimi H, Nikbakht AM, Najafi G and Yusaf TF. Diesel engine performance and exhaust emission analysis using waste cooking biodiesel fuel with an artificial neural network. *Renew Energy* 2009; 34: 976–982.
- Chauhan BS, Kumar N and Cho HM. A study on the performance and emission of a diesel engine fueled with *Jatropha* biodiesel oil and its blends. *Energy* 2012; 37: 616–622.
- Karami R, Rasul MG, Khan MMK, Mahdi Salahi M and Anwar M. Experimental and computational analysis of combustion characteristics of a diesel engine fueled with diesel-tomato seed oil biodiesel blends. *Fuel* 2021; 285: 1–13.
- Bishop D, Situ R, Brown R and Surawski N. Numerical modelling of biodiesel blends in a diesel engine. *Energy Proc* 2017; 110: 402–407.
- Asadi A, Kadijani ON, Doranehgard MH, et al. Numerical study on the application of biodiesel and bioethanol in a multiple injection diesel engine. *Renew Energy* 2020; 150: 1019–1029.
- Hassan NM, Rasul MG and Harch CA. Modelling and experimental investigation of engine performance and emissions fuelled with biodiesel produced from Australian beauty leaf tree. *Fuel* 2015; 150: 625–635.
- Karami R, Rasul M and Khan M. CFD simulation and a pragmatic analysis of performance and emissions of

- tomato seed biodiesel blends in a 4-Cylinder diesel engine. *Energies* 2020; 13(14): 1–20.
19. Aksoy F, Uyumaz A, Boz F and Yılmaz E. Experimental investigation of neutralized waste cooking oil biodiesel/diesel mixture and diesel fuel in a diesel engine at different engine loads. *Int J Automot Sci Technol* 2017; 1(1): 7–15.
  20. Salehian A and Shirneshan A. The effect of cordierite-platinum SCR catalyst on the NOx removal efficiency in an engine fueled with diesel-ethanol-biodiesel blends. *Catal Lett* 2020; 150: 2236–2253.
  21. Farajollahi A and Firuzi R. Numerical investigation on the effect creating groove inside the injector nozzle on the spray behavior of diesel and biodiesel fuels. *Aerosp Knowl Technol J* 2020; 9(2): 1–6.
  22. Lešnik L, Vajda B, Žunič Z, Škerget L and Kegl B. The influence of biodiesel fuel on injection characteristics, diesel engine performance, and emission formation. *Appl Energy* 2013; 111: 558–570.
  23. Moldovanu D and Burnete N. Computational fluid dynamics simulation of a single cylinder research engine working with biodiesel. *Therm Sci* 2013; 17(1): 195–203.
  24. Ni P, Wei D, Wang X, Zhang D and Wang Z. Suppression of soot of a diesel engine fueled with biodiesel-diesel blends. *Sustain Energy* 2015; 34(1): 282–288.
  25. Merish S, Tamizhamuthu M and Walter TM. Review of shorea robusta with special reference to traditional siddha medicine. *Res Rev J Pharmacognosy Phytochem* 2014; 2(1): 5–13.
  26. Shashi CK, Pradhan CM, Ghosh P, Rana SS and Mishra S. Shorea robusta (Dipterocarpaceae) seed and its oil as food. *Int J Food Nutr Sci* 2015; 4(4): 228–233.
  27. Alam M, Furukawa Y, Sarker SK and Ahmed R. Sustainability of sal (*Shorea robusta*) forest in Bangladesh: past, present and future actions. *Int For Rev* 2008; 10(1): 29–37.
  28. Hasan MI, Mukta NA, Islam MM, Chowdhury AMS and Ismail M. Evaluation of fuel properties of Sal (*Shorea robusta*) seed and its oil from their physico-chemical characteristics and thermal analysis. *Energy Sources A Recovery Util Environ Eff* 2020; 1–12. DOI: 10.1080/15567036.2020.1774684
  29. Pali HS, Kumar N and Alhassan Y. Performance and emission characteristics of an agricultural diesel engine fueled with blends of Sal methyl esters and diesel. *Energy Convers Manag* 2015; 90: 146–153.
  30. Vedaraman N, Puhan S, Nagarajan G, Ramabrahmam BV and Velappan KC. Methyl ester of Sal oil (*Shorea robusta*) as a substitute to diesel fuel—A study on its preparation, performance and emissions in direct injection diesel engine. *Ind Crops Prod* 2012; 36(1): 282–288.
  31. Pali HS and Kumar N. Combustion, performance and emissions of Shorea robusta methyl ester blends in a diesel engine. *Biofuels* 2016; 7(5): 447–456.
  32. Pali HS and Kumar N. Comparative assessment of sal methyl ester and kumum methyl ester with diesel in CI engine. In: *Vth international symposium on "fusion of science & technology,"* New Delhi, India, 18–22 January 2016.
  33. Chen Y, Li X, Li X, Zhao W and Liu F. The wall-flow-guided and interferential interactions of the lateral swirl combustion system for improving the fuel/air mixing and combustion performance in DI diesel engines. *Energy* 2019; 166: 690–700.
  34. Şener R, Özdemir MR and Yangaz MU. Influence of piston bowl geometry on combustion and emission characteristics. *Proc IMechE Part A: J Power and Energy* 2019; 233(5): 576–587.
  35. Gokbel R. *Modernization of the antor 3LD 510 diesel engine applying of the new (MR-1) single swirl type combustion chamber and intake port geometry.* MSc thesis, Istanbul Technical University, Institute of Science and Technology, Istanbul, Turkey, 2008.
  36. Kavruk KO. *Investigation of using the MRI combustion chamber and the effects to the in-cylinder parameters and performance on the antor 3LD 510 diesel engine.* MSc thesis, Istanbul Technical University, Institute of Science and Technology, Istanbul, Turkey, 2008.
  37. Mehdiyev R, Alkan AD, Unar M and Karatas O. An alternative superior combustion mechanism that can convert domestic production marine diesel engines to 100% natural gas fuels. *GMO J Ship Mar Technol* 2017; 23(207): 49–65.
  38. Mehdiyev R, Ogun K, Ozcan E, Arslan H, Babaoglu O and Teker H. The twin swirl “MR-Process” combustion mechanism and conversion of diesel engines to operate with gaseous fuels. SAE paper 2011-24-0066, 2011, pp. 1–11. DOI: 10.4271/2011-24-0066
  39. Ganji PR, Singh RN, Raju VRK and Srinivasa Rao S. Design of piston bowl geometry for better combustion in direct-injection compression ignition engine. *Sadhana J* 2018; 92: 1–9.
  40. Khan S, Panua R and Bose PK. Combined effects of piston bowl geometry and spray pattern on mixing, combustion and emissions of a diesel engine: a numerical approach. *Fuel* 2018; 225: 203–217.
  41. Li X, Chen Y, Su L and Liu F. Effects of lateral swirl combustion chamber geometries on the combustion and emission characteristics of DI diesel engines and a matching method for the combustion chamber geometry. *Fuel* 2018; 224: 644–660.
  42. Wei S, Wang F, Leng X, Liu X and Ji K. Numerical analysis on the effect of swirl ratios on swirl chamber combustion system of DI diesel engines. *Energy Convers Manag* 2013; 75: 184–190.
  43. <https://www.biodiesel.org/using-biodiesel/buying-guide>, 2022, The national biodiesel board is now clean fuels alliance America. Accessed 10 December 2022.
  44. Temizer İ and Eskici B. Investigation on the combustion characteristics and lubrication of biodiesel and diesel fuel used in a diesel engine. *Fuel* 2020; 278: 1–10.
  45. Harch CA, Rasul MG, Hassan NM and Bhuiya MM. Modelling of engine performance fuelled with second generation biodiesel. *Procedia Eng* 2014; 90: 459–465.
  46. Hisham S, Kadrigama K, Ramasamy D, et al. Waste cooking oil blended with the engine oil for reduction of friction and wear on piston skirt. *Fuel* 2017; 205: 247–261.
  47. Abed KA, Gad MS, El Morsi AK, Sayed MM and Elyazeed SA. Effect of biodiesel fuels on diesel engine emissions. *Egypt J Pet* 2019; 28(2): 183–188.
  48. Aldhaidhawi M, Brabec M, Lucian M, Chiriac R and Bădescu V. Experimental and numerical assessment of ignition delay period for pure diesel and biodiesel B20. *IOP Conf Ser Mater Sci Eng* 2017; 252: 012068.
  49. Dhar A and Agarwal AK. Experimental investigations of effect of Karanja biodiesel on tribological properties of lubricating oil in a compression ignition engine. *Fuel* 2014; 130: 112–119.

50. E J, Liu T, Yang WM, Li J, Gong J and Deng Y. Effects of fatty acid methyl esters proportion on combustion and emission characteristics of a biodiesel fueled diesel engine. *Energy Convers Manag* 2016; 117: 410–419.
51. Temizer İ and Cihan Ö. Analysis of different combustion chamber geometries using hydrogen / diesel fuel in a diesel engine. *Energy Sources A Recovery Util Environ Eff* 2021; 43(1): 17–34.
52. Cihan Ö. Experimental and numerical investigation of the effect of fig seed oil methyl ester biodiesel blends on combustion characteristics and performance in a diesel engine. *Energy Rep* 2021; 7: 5846–5856.
53. Soni DK and Gupta R. Numerical analysis of flow dynamics for two piston bowl designs at different spray angles. *J Clean Prod* 2017; 149: 723–734.
54. Soni DK and Gupta R. Numerical investigation of emission reduction techniques applied on methanol blended diesel engine. *Alex Eng J* 2016; 55: 1867–1879.
55. Pali HS, Mishra C, Yahaya A and Sidharth Kumar N. Sal Seed oil: a potential feedstock for biodiesel production. In: *ISTE Delhi section convention conference*, Delhi, India, 5–6 September 2013, Delhi Technological University.
56. López JJ, Novella R, García A and Winklinger JF. Investigation of the ignition and combustion processes of a dual-fuel spray under diesel-like conditions using computational fluid dynamics (CFD) modeling. *Math Comput Model* 2013; 57: 1897–1906.
57. Dueso C, Muñoz M, Moreno F, et al. Performance and emissions of a diesel engine using sunflower biodiesel with a renewable antioxidant additive from bio-oil. *Fuel* 2018; 234: 276–285.
58. Chowdry SS and Raj CS. Study of physical and chemical properties of cardanol ethyl ester for its suitability as petro-diesel. *Int J Chem Sci* 2017; 15(1): 413–427.
59. Baweja S, Trehan A and Kumar R. Combustion, performance, and emission analysis of a CI engine fueled with mustard oil biodiesel blended in diesel fuel. *Fuel* 2021; 292: 1–12.
60. Kattela SP, Vysyaraju RKR, Surapaneni SR and Ganji PR. Effect of n-butanol/diesel blends and piston bowl geometry on combustion and emission characteristics of CI engine. *Environ Sci Pollut Res* 2019; 26(2): 1661–1674.
61. SivaPrasad K, Rao SS and Raju VRK. Enhancement of mixture homogeneity for DI-CI engine to achieve homogeneous charge compression ignition (HCCI) combustion characteristics: a numerical approach. *Energy Sources A Recovery Util Environ Eff* 2022; 44(2): 4318–4333.
62. Temizer İ and Cihan Ö. Heat and flow analysis of different piston bowl geometries in a diesel engine. *Int J Automot Sci Technol* 2021; 5(3): 206–213.
63. Guo Z, He X, Pei Y, et al. Optimization of piston bowl geometry for a low emission heavy-duty diesel engine. *SAE technical paper 2020-01-2056*, 2020, pp.1–18. DOI: 10.4271/2020-01-2056

## Appendix

### Notation

ATDC	After Top Dead Center
B10	10% Sal Seed Oil Methyl Ester + 90% Diesel Fuel
CA	Crank Angle
CFD	Computational Fluid Dynamic
DI	Direct Injection
ID	Ignition Delay
MCC	Modified Combustion Chamber
NHRR	Net Heat Release Rate
SCC	Standard Combustion Chamber
TDC	Top Dead Center